Lasers in Eng., Vol. 1, pp. 135–151
Reprints available directly from the publisher
Photocopying permitted by license only

Orbital Angular Momentum Density of an Elegant Laguerre-Gaussian Laser Beam in the Source Region

Y-M. ZHOU AND G-Q. ZHOU*

School of Sciences, Zhejiang A & F University, Lin'an 311300, Zhejiang Province, China

Based on the method of the vectorial angular spectrum of a laser beam, an analytical expression of the electric field of an elegant Laguerre-Gaussian laser beam in source region is derived without any approximation, and the corresponding magnetic field is obtained by taking the curl of the electric field. By using the obtained expressions of the electromagnetic fields, the orbital angular momentum density of the elegant Laguerre-Gaussian laser beam can be accurately calculated. The effects of the angular mode number, the radial mode number and the linearly polarized angle as well as the beam waist width on the distribution of the orbital angular momentum density of the elegant Laguerre-Gaussian laser beam are investigated, respectively. Also, the orbital angular momentum density distribution of the propagating part of the elegant Laguerre-Gaussian laser beam is compared with that of the whole laser beam. Upon propagation, the orbital angular momentum density difference between the propagating part and the whole laser beam decreases. This research is beneficial to the optical manipulation with an elegant Laguerre-Gaussian laser beam.

Keywords: Elegant Laguerre-Gaussian laser beam, orbital angular momentum density, source region, propagating part, evanescent part

1 INTRODUCTION

An elegant Laguerre-Gaussian laser beam is an extension of the standard Laguerre-Gaussian laser beam [1]. Higher–order complex source has been proposed to generate the elegant Laguerre–Gaussian laser beams [2]. An exact closed-form representation of a vector elegant Laguerre-Gaussian wave

*Corresponding author: Tel: +86 (0)571 6374 0072; E-mail: 1911645003@qq.com

packet has been derived [3]. Vortex and anti–vortex compositions of exact elegant Laguerre-Gaussian vector laser beams have been expressed in a closed analytic form [4].

Elegant Laguerre-Gaussian laser beams can be used to describe the axi-symmetric flattened Gaussian laser beam [5]. The relationship between the elegant Laguerre-Gaussian and the Bessel-Gaussian laser beams has been illuminated [6]. The propagating properties of the elegant Laguerre-Gaussian laser beams in free space [7–9], in turbulent atmosphere [10], in non–Kolmogorov turbulence [11], in a uniaxial crystal [12], at a dielectric interface [13], by an opaque obstacle [14], through a paraxial *ABCD* optical system [15], through aligned and misaligned paraxial optical systems [16, 17] and in apertured fractional Hankel transform systems [18], have all been investigated.

The vectorial structure of the elegant Laguerre–Gaussian laser beam has been demonstrated in the far–field regime [19]. New fractional–order solutions of the paraxial wave equation have been introduced, which smoothly connect the elegant Laguerre–Gaussian laser beams of integral–order [20]. As the angular mode index changes continuously between integer values, the transition of the vortex structure of fractional elegant Laguerre-Gaussian laser beams has been analysed in detail [21]. The elegant Laguerre–Gaussian laser beams can also be extended to the nonparaxial [22, 23] and the partially coherent cases [24–29].

The major advantage of an elegant Laguerre-Gaussian laser beam is that it carries the orbital angular momentum. This leads one to focus on studying the orbital angular momentum. For instance, the compact expression for the derivatives of an elegant Laguerre- Gaussian laser beam has been presented to study the resulting orbital angular momentum and phase structure [30]. The expression of the orbital angular momentum density of the elegant Laguerre-Gaussian laser beam has been derived [31], which is applicable to both the near and far fields. According to the value of the axial propagation distance z, the beam propagation region is divided into three regions [32]: the source region where z is less than or comparable to the optical wavelength, the near-field where z is larger than a few wavelengths, and the far field where z approaches to infinity. Among them, one may be more curious to know the orbital angular momentum density distribution of the elegant Laguerre-Gaussian laser beam in the source region, which is just the purpose of this paper.

As the overall transverse component of the orbital angular momentum is zero, here only the longitudinal component of the orbital angular momentum density is considered. The effects of the beam parameters on the orbital angular momentum density distribution of the elegant Laguerre-Gaussian laser beam in the source region are discussed. Also, the orbital angular momentum density distribution of the propagating part of the elegant Laguerre-Gaussian laser beam is compared with that of the whole beam.

2 ORBITAL ANGULAR MOMENTUM DENSITY OF AN ELEGANT LAGUERRE-GAUSSIAN LASER BEAM IN THE SOURCE REGION

In the cylindrical coordinate system, the z–axis is taken to be the propagation axis. The elegant Laguerre-Gaussian laser beam is assumed to be linearly polarized. The elegant Laguerre-Gaussian laser beam in the source plane $z = 0$ takes the form as

$$\begin{bmatrix} E_x(\rho,0,\theta) \\ E_y(\rho,0,\theta) \end{bmatrix} = \begin{bmatrix} \cos\alpha \\ \sin\alpha \end{bmatrix} \left(\frac{\rho}{w_0}\right)^m L_n^m\left(\frac{\rho^2}{w_0^2}\right) \exp\left(-\frac{\rho^2}{w_0^2}\right) \exp(im\theta) \tag{1}$$

where w_0 is the Gaussian waist size, and L_n^m is the associated Laguerre polynomial. n and m are the radial and angular mode numbers, respectively. $\rho = (x^2+y^2)^{1/2}$ and $\theta = \arctan(y/x)$. $\begin{pmatrix} \cos\alpha \\ \sin\alpha \end{pmatrix}$ describes the linearly polarized state, and α is the linearly polarized angle. The time dependent factor $\exp(-i\omega t)$ is omitted in the equation (1), and ω is the angular frequency. The exact description of the elegant Laguerre-Gaussian laser beam should be directly initiated from Maxwell's equations. Moreover, the method of the vectorial angular spectrum is used to resolve Maxwell's equations. Therefore, the propagating electric field of the elegant Laguerre-Gaussian laser beam in the source region can be expressed in the form of the vectorial angular spectrum [33]:

$$\boldsymbol{E}(\rho,z,\theta) = \int_0^\infty \int_0^{2\pi} \left\{ A_x(b,\varphi)\left(\mathbf{e}_x - \frac{b\cos\varphi}{\gamma}\mathbf{e}_z\right) + A_y(b,\varphi)\left(\mathbf{e}_y - \frac{b\sin\varphi}{\gamma}\mathbf{e}_z\right)\right\}$$
$$\times\ \exp\{ik[b\rho\cos(\varphi-\theta)+\gamma z]\} b\,db\,d\varphi \tag{2}$$

where $b^2 = (p^2+q^2)^{1/2}; \gamma = (1-b^2)^{1/2};\ \varphi = \arctan(q/p)$; $\mathbf{e}_x$, $\mathbf{e}_y$ and $\mathbf{e}_z$ are the three unit vectors in the x-, y-, and z-directions, respectively; p/λ and q/λ are the transverse frequencies; and $A_x(b,\varphi)$ and $A_y(b,\varphi)$ are the x- and y-components of the vectorial angular spectrum. $A_x(b,\varphi)$ is given by the Fourier transformation of the x-component of initial electric field [34]:

$$A_x(b,\varphi) = \frac{\cos\alpha}{\lambda^2}\int_0^\infty \int_0^{2\pi} \left(\frac{\rho'}{w_0}\right)^m L_n^m\left(\frac{\rho'^2}{w_0^2}\right)\exp\left(-\frac{\rho'^2}{w_0^2}\right)$$
$$\times \exp[im\theta' - ikb\rho'\cos(\theta'-\varphi)]\rho' d\rho' d\theta' \tag{3}$$

We recall the following mathematical formulae [34]:

$$\int_0^{2\pi} \exp[im\theta' - ikb\rho' \cos(\theta' - \varphi)]d\theta' = 2\pi(-i)^m J_m(kb\rho')\exp(im\varphi) \quad (4)$$

$$L_n^m\left(\frac{\rho'^2}{w_0^2}\right) = \sum_{l=0}^{n} \frac{(-1)^l}{l!}\binom{n+m}{n-l}\frac{\rho'^{2l}}{w_0^{2l}} \quad (5)$$

$$\int_0^{\infty} \frac{\rho'^{2l+m}}{w_0^{2l+m}} J_m(kb\rho')\exp\left(-\frac{\rho'^2}{w_0^2}\right)\rho' d\rho' = \frac{w_0^2 l!}{2}\left(\frac{b}{2f}\right)^m \times \exp\left(-\frac{b^2}{4f^2}\right)L_l^m\left(\frac{b^2}{4f^2}\right) \quad (6)$$

where J_m is the m^{th} order Bessel function of the first kind and $f = 1/(kw_0)$. $k = 2\pi/\lambda$ is the wave number. The x-component of the vectorial angular spectrum is found to be

$$A_x(b,\varphi) = \frac{(-i)^m \cos\alpha}{4\pi f^2}\exp(im\varphi)\sum_{l=0}^{n}(-1)^l\binom{n+m}{n-l} \times\left(\frac{b}{2f}\right)^m \exp\left(-\frac{b^2}{4f^2}\right)L_l^m\left(\frac{b^2}{4f^2}\right) \quad (7)$$

The y-component of the vectorial angular spectrum yields

$$A_y(b,\varphi) = \frac{(-i)^m \sin\alpha}{4\pi f^2}\exp(im\varphi)\sum_{l=0}^{n}(-1)^l\binom{n+m}{n-l}\left(\frac{b}{2f}\right)^m \times\exp\left(-\frac{b^2}{4f^2}\right)L_l^m\left(\frac{b^2}{4f^2}\right) \quad (8)$$

The x–component of the optical field of the elegant Laguerre–Gaussian laser beam in the source region yields

$$E_x(\rho,z,\theta) = \cos\alpha\exp(im\theta)\sum_{l=0}^{n}\sum_{s=0}^{l}\frac{(-1)^{l+s}}{2^{2s+m+1}f^{2s+m+2}s!}\binom{n+m}{n-l} \times\binom{l+m}{l-s}\int_0^{\infty} b^{2s+m}\exp\left(-\frac{b^2}{4f^2}\right)J_m(kb\rho)\exp(ik\gamma z)b\,db \quad (9)$$

By transforming the integral variable from b to γ, Equation (9) can be rewritten as

$$\begin{aligned} E_x(\rho, z, \theta) &= \cos\alpha \exp\left(-\frac{1}{4f^2} + im\theta\right) \\ &\times \sum_{l=0}^{n}\sum_{s=0}^{l} \frac{(-1)^{l+s}}{2^{2s+m+1} f^{2s+m+2} s!} \binom{n+m}{n-l}\binom{l+m}{l-s} \\ &\times \left(\int_0^1 - \int_0^{+i\infty}\right) b^{2s+m} J_m\left(k\rho\sqrt{1-\gamma^2}\right) \exp\left(\frac{\gamma^2}{4f^2}\right) \exp(ik\gamma z)\gamma d\gamma \end{aligned} \tag{10}$$

As the integration is inconvenient to perform, one can consider the following Taylor expansions [34]

$$b^{2s+m} J_m\left(k\rho\sqrt{1-\gamma^2}\right) = \sum_{u=0}^{\infty}\sum_{v=0}^{m+s+u} \frac{(-1)^{u+v}(m+s+u)!(k\rho)^{m+2u}\gamma^{2v}}{2^{m+2u} u! v! (m+u)! (m+s+u-v)!} \tag{11}$$

The x-component of the optical field of the elegant Laguerre-Gaussian laser beam in the source region turns out to be

$$\begin{aligned} E_x(\rho, z, \theta) &= \cos\alpha \exp\left(-\frac{1}{4f^2} + im\theta\right) \\ &\times \sum_{l=0}^{n}\sum_{s=0}^{l}\sum_{u=0}^{\infty}\sum_{v=0}^{m+s+u} \frac{(-1)^{l+s+u+v}(m+s+u)!(k\rho)^{m+2u}}{2^{2(s+m+u)+1} f^{2s+m+2} s! u! v! (m+u)! (m+s+u-v)!} \\ &\times \binom{n+m}{n-l}\binom{l+m}{l-s}\left(\int_0^1 - \int_0^{+i\infty}\right) \exp\left(\frac{\gamma^2}{4f^2}\right) \exp(ik\gamma z)\gamma^{2v+1} d\gamma \end{aligned} \tag{12}$$

To obtain the analytical expression, we first perform the propagation term [34]

$$\begin{aligned} I_j^{\text{pro}} &= \int_0^1 \exp\left(\frac{\gamma^2}{4f^2}\right) \exp(ik\gamma z)\gamma^j d\gamma = 2f^2 \\ &\times \left[\exp\left(\frac{1}{4f^2} + ikz\right) - ikz I_{j-1}^{\text{pro}} - (j-1) I_{j-2}^{\text{pro}}\right] \end{aligned} \tag{13}$$

with I_0^{pro} and I_1^{pro} being given by

$$I_0^{\mathrm{pro}} = if\sqrt{\pi}\left[F\left(\frac{iz}{w_0}\right) - \exp\left(\frac{1}{4f^2} + ikz\right)F\left(\frac{iz}{w_0} + \frac{kw_0}{2}\right)\right] \tag{14}$$

$$I_1^{\mathrm{pro}} = 2f^2\left[\exp\left(\frac{1}{4f^2} + ikz\right) - 1 - ikzI_0^{\mathrm{pro}}\right] \tag{15}$$

where j is an arbitrary integer and $F(\cdot)$ is the Faddeev function [35]. Secondly, the evanescent term yields [34]

$$I_j^{\mathrm{eva}} = \int_0^{+i\infty} \exp\left(\frac{\gamma^2}{4f^2}\right)\exp(ik\gamma z)\gamma^j d\gamma = \left(i\sqrt{2}f\right)^{j+1} j!D_{j+1}\left(\frac{\sqrt{2}z}{w_0}\right) \tag{16}$$

where $D_{j+1}(\cdot)$ is related to the parabolic cylinder function. The recurrence relation of $D_{j+1}(\cdot)$ is found to be [33]

$$D_1\left(\frac{\sqrt{2}z}{w_0}\right) = \sqrt{\frac{\pi}{2}}F\left(\frac{iz}{w_0}\right) \tag{17}$$

$$D_2\left(\frac{\sqrt{2}z}{w_0}\right) = 1 - \frac{\sqrt{2}z}{w_0}D_1\left(\frac{\sqrt{2}z}{w_0}\right) \tag{18}$$

$$D_{j+1}\left(\frac{\sqrt{2}z}{w_0}\right) = \frac{1}{j}\left[D_{j-1}\left(\frac{\sqrt{2}z}{w_0}\right) - \frac{\sqrt{2}z}{w_0}D_j\left(\frac{\sqrt{2}z}{w_0}\right)\right] \tag{19}$$

Finally, the x-component of the optical field of the elegant Laguerre–Gaussian laser beam in the source region can be analytically expressed as

$$\begin{aligned}
&E_x(\rho, z, \theta) = E_x^{\mathrm{pro}}(\rho, z, \theta) + E_x^{\mathrm{eve}}(\rho, z, \theta) \\
&= \cos\alpha \exp\left(-\frac{1}{4f^2} + im\theta\right) \\
&\times \sum_{l=0}^{n}\sum_{s=0}^{l}\sum_{u=0}^{\infty}\sum_{v=0}^{m+s+u} \frac{(-1)^{l+s+u+v}(m+s+u)!(k\rho)^{m+2u}}{2^{2(s+m+u)+1}f^{2s+m+2}s!u!v!(m+u)!(m+s+u-v)!} \\
&\times \binom{n+m}{n-l}\binom{l+m}{l-s}\left(I_{2v+1}^{\mathrm{pro}} - I_{2v+1}^{\mathrm{eva}}\right)
\end{aligned} \tag{20}$$

where $E_x^{\text{pro}}(\rho, z, \theta)$ and $E_x^{\text{eve}}(\rho, z, \theta)$ denote the propagating and the evanescent parts, respectively. The y–component of the optical field of the elegant Laguerre–Gaussian laser beam in the source region turns out to be

$$
\begin{aligned}
E_y(\rho, z, \theta) &= E_y^{\text{pro}}(\rho, z, \theta) + E_y^{\text{eve}}(\rho, z, \theta) \\
&= \sin\alpha \exp\left(-\frac{1}{4f^2} + im\theta\right) \\
&\times \sum_{l=0}^{n}\sum_{s=0}^{l}\sum_{u=0}^{\infty}\sum_{v=0}^{m+s+u} \frac{(-1)^{l+s+u+v}(m+s+u)!(k\rho)^{m+2u}}{2^{2(s+m+u)+1} f^{2s+m+2} s!u!v!(m+u)!(m+s+u-v)!} \\
&\times \binom{n+m}{n-l}\binom{l+m}{l-s}\left(I_{2v+1}^{\text{pro}} - I_{2v+1}^{\text{eva}}\right)
\end{aligned} \tag{21}
$$

The longitudinal component of the optical field of the elegant Laguerre–Gaussian laser beam in the source region reads as

$$
\begin{aligned}
E_z(\rho, z, \theta) &= E_z^{\text{pro}}(\rho, z, \theta) + E_z^{\text{eve}}(\rho, z, \theta) \\
&= -\frac{i\cos(\theta-\alpha)}{2f^{2s+m+2}} \exp\left(-\frac{1}{4f^2} + im\theta\right) \\
&\times \sum_{l=0}^{n}\sum_{s=0}^{l}\sum_{u=0}^{\infty}\sum_{v=0}^{m+s+u+1} \frac{(-1)^{l+s+u+v}(m+s+u+1)!(k\rho)^{m+2u+1}}{2^{2(s+m+u)+1} s!u!v!(m+u+1)!(m+s+u+1-v)!} \\
&\times \binom{n+m}{n-l}\binom{l+m}{l-s}\left(I_{2v}^{\text{pro}} - I_{2v}^{\text{eva}}\right)
\end{aligned} \tag{22}
$$

According to Maxwell's equations, the magnetic field of the elegant Laguerre–Gaussian laser beam in the source region turns out to be

$$
\boldsymbol{H}(\rho, z, \theta) = \frac{i}{\omega\mu_0} \nabla \times \boldsymbol{E}(\rho, z, \theta) \tag{23}
$$

where μ_0 is the magnetic permeability of vacuum. The Poyting vector of the elegant Laguerre–Gaussian laser beam in the source region is given by

$$
\boldsymbol{S}(\rho, z, \theta) = \frac{1}{4} < \boldsymbol{E}(\rho, z, \theta) \times \boldsymbol{H}^*(\rho, z, \theta) + \boldsymbol{E}^*(\rho, z, \theta) \times \boldsymbol{H}(\rho, z, \theta) > \tag{24}
$$

where the angle brackets indicate an average with respect to the time, and the asterisk denotes the complex conjugation. Therefore, the orbital angular momentum density of the elegant Laguerre–Gaussian laser beam in the source region is found to be [36, 37]

$$J_z(\rho, z, \theta) = \varepsilon_0 \mu_0 [\boldsymbol{r} \times \boldsymbol{S}(\rho, z, \theta)]_z \tag{25}$$

where $\boldsymbol{r} = x\mathbf{e}_x + y\mathbf{e}_y + z\mathbf{e}_z$ and ε_0 is the electric permittivity of vacuum.

3 NUMERICAL CALCULATIONS AND ANALYSES

The orbital angular momentum density of the elegant Laguerre–Gaussian laser beam in a reference plane is determined by the angular mode number, the radial mode number and the linearly polarized angle as well as the beam waist width. Now, the effect of the angular mode number on the distribution of the orbital angular momentum density is investigated firstly, as shown in Figure 1. $w_0 = \lambda/2$, $n = 3$, $\alpha = 0$, and $z = \lambda/16$ in Figure 1. When $m = 0$, the orbital angular momentum density is composed of five layers. Each layer has four lobes. Both the areas and the magnitude of the positive and the negative angular momentum densities are equivalent. Therefore, the overall angular momentum density in the reference plane is zero. When $m > 0$, the distribution of the orbital angular momentum density is composed of two symmetrical lobes, which are located in the horizontal direction. With the angular mode number increasing, the magnitude of the orbital angular momentum density increases rapidly, and the pattern size of the orbital angular momentum density also slowly augments. The shape of the distribution of the orbital angular momentum density also slightly changes with the angular mode number.

Figure 2 represents the influence of the radial mode number on the distribution of the orbital angular momentum density. $w_0 = \lambda/2$, $m = 2$, $\alpha = 0$, and $z = \lambda/16$ in Figure 2. With the increasing in a radial mode number, the magnitude of the orbital angular momentum density increases, but the pattern size of the orbital angular momentum density decreases. The shape of the distribution of the orbital angular momentum density also changes slightly with the increase of radial mode number.

Figure 3 denotes the effect of linearly polarized angle on the shape, the location, and the magnitude of the distribution of the orbital angular momentum density. $m = 2$, $n = 3$, $w_0 = \lambda/2$, and $z = \lambda/16$ in Figure 3. When the linearly polarized angle varies, the change in the shape of the distribution of the orbital angular momentum density is not very apparent. When $\alpha = 0$, the distribution of the orbital angular momentum density is located at the x-axis, as shown in Figure 3. As the linearly polarized angle increases, the distribution of the orbital angular momentum density rotates anticlockwise and its rota-

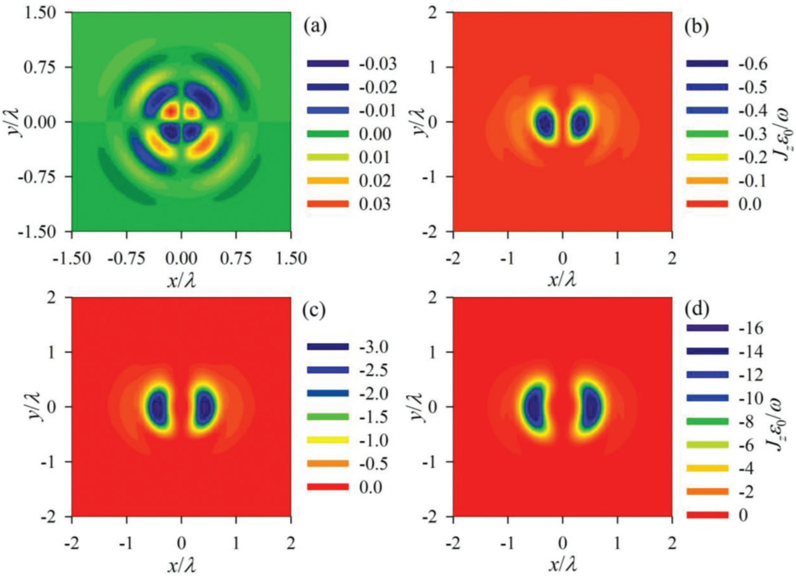

FIGURE 1
The orbital angular momentum density of the elegant Laguerre-Gaussian laser beam in the reference plane $z = \lambda/16$. $w_0 = \lambda/2$, $n = 3$, and $\alpha = 0$. (a) $m = 0$. (b) $m = 1$. (c) $m = 2$. (d) $m = 3$.

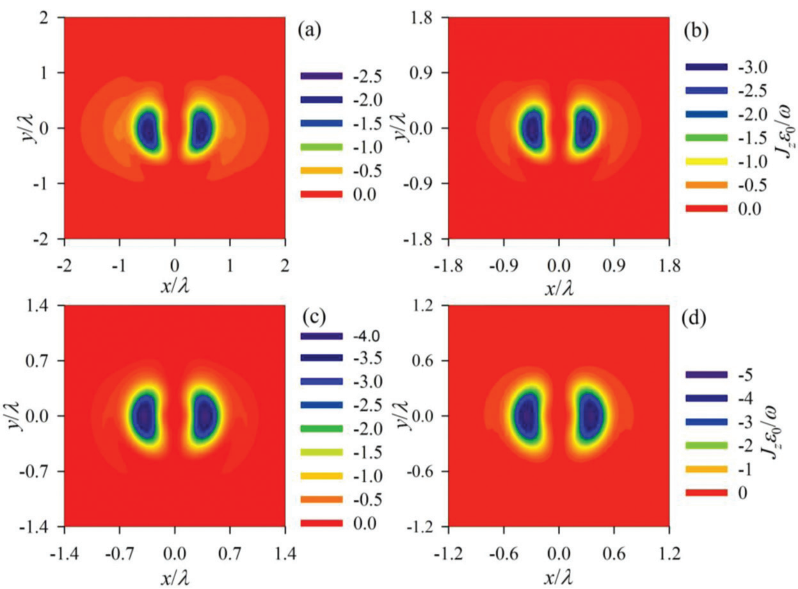

FIGURE 2
The orbital angular momentum density of the elegant Laguerre-Gaussian laser beam in the reference plane $z = \lambda/16$. $w_0 = \lambda/2$, $m = 2$, and $\alpha = 0$. (a) $n = 2$. (b) $n = 3$. (c) $n = 4$. (d) $n = 5$.

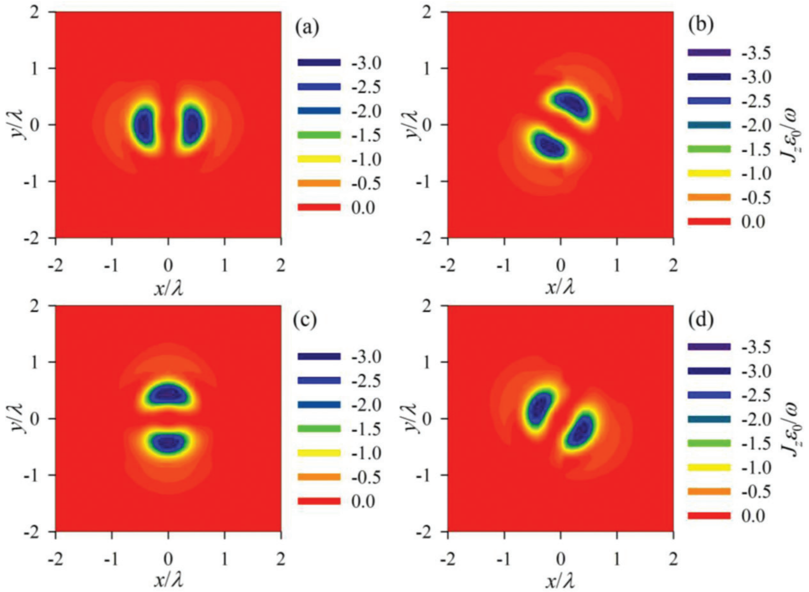

FIGURE 3
The orbital angular momentum density of the elegant Laguerre-Gaussian laser beam in the reference plane $z = \lambda/16$. $w_0 = \lambda/2$, $m = 2$, and $n = 3$. (a) $\alpha = 0$. (b) $\alpha = \pi/3$. (c) $\alpha = \pi/2$. (d) $\alpha = 5\pi/6$.

tion angle is the same as the linearly polarized angle. The magnitude of the orbital angular momentum density in the two cases of $\alpha = 0$ and $\alpha = \pi/2$ are smaller than that in the other two cases of $\alpha = \pi/3$ and $\alpha = 5\pi/6$. Figure 4 shows the effect of the beam waist width on the distribution of the orbital angular momentum density. $m = 2$, $n = 3$, $\alpha = 0$, and $z = \lambda/16$ in Figure 4. Both the magnitude and the pattern size of the orbital angular momentum density increase with the increase of beam waist width. As the beam waist width varies, the shape of the distribution of the orbital angular momentum density also changes.

The orbital angular momentum density of the elegant Laguerre-Gaussian laser beam in the different reference plane is shown in Figure 5. $w_0 = \lambda/2$, $m = 2$, $n = 3$, and $\alpha = 0$ in Figure 5. Upon propagation, the profile of the distribution of orbital angular momentum density expands, and the magnitude of the orbital angular momentum density decreases. Moreover, the shape of the distribution of the orbital angular momentum density changes obviously at first, and then tends to be stable during propagation.

Figure 6 represents the orbital angular momentum density of the propagating part of the elegant Laguerre-Gaussian laser beam in the reference plane $z = \lambda/16$. $w_0 = \lambda/2$, $n = 3$, and $\alpha = 0$ in Figure 6. By comparing Figure 6 with Figure 1, the magnitude of the orbital angular momentum density of the propagating part of the elegant Laguerre-Gaussian laser beam is far smaller than

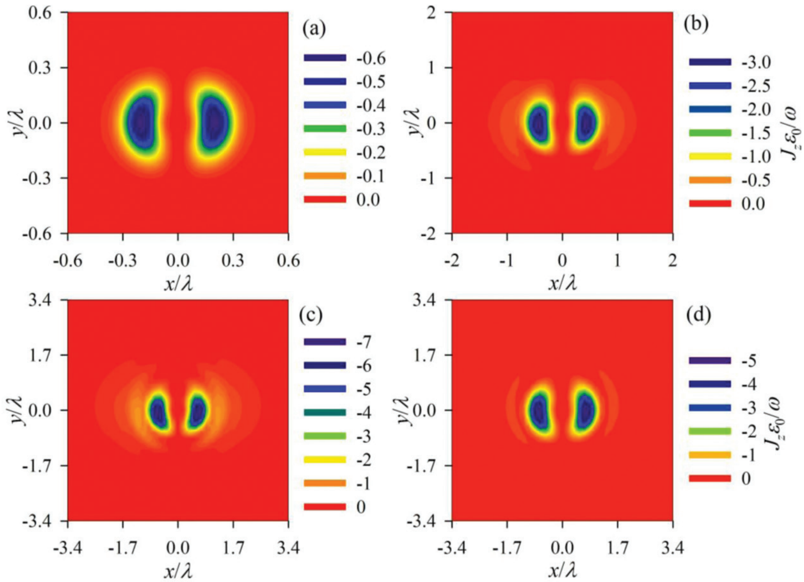

FIGURE 4
The orbital angular momentum density of the elegant Laguerre-Gaussian laser beam in the reference plane $z = \lambda/16$. $m = 2$, $n = 3$, and $\alpha = 0$. (a) $w_0 = \lambda/4$. (b) $w_0 = \lambda/2$. (c) $w_0 = 3\lambda/4$. (d) $w_0 = \lambda$.

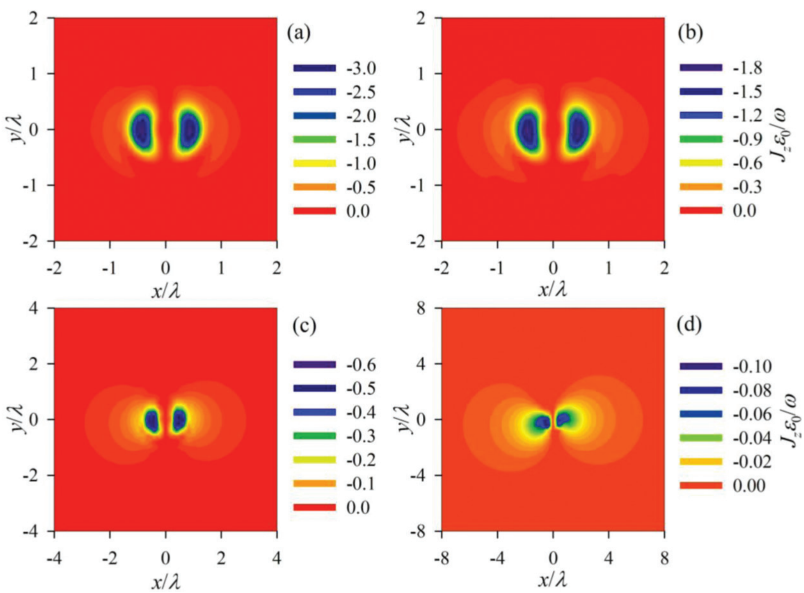

FIGURE 5
The orbital angular momentum density of the elegant Laguerre-Gaussian laser beam in the different reference planes. $w_0 = \lambda/2$, $m = 2$, $n = 3$, and $\alpha = 0$. (a) $z = \lambda/16$. (b) $z = \lambda/8$. (c) $z = \lambda/4$. (d) $z = \lambda/2$.

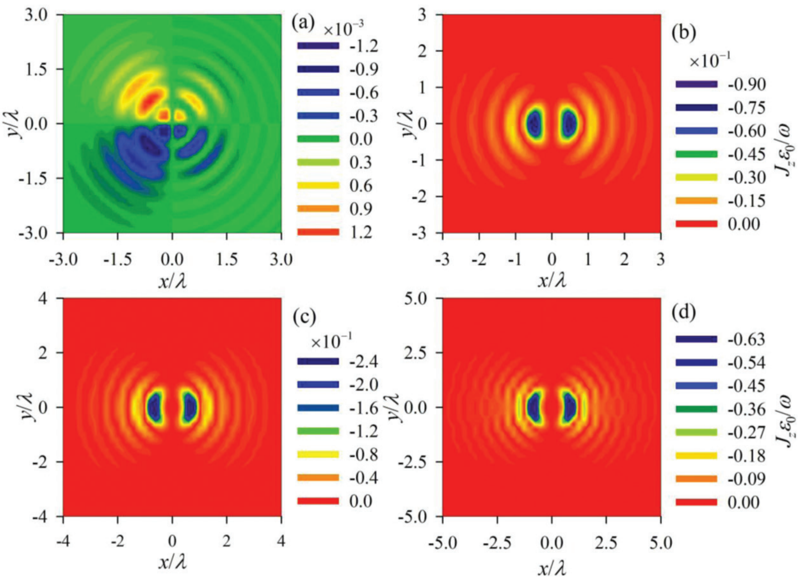

FIGURE 6
The orbital angular momentum density of the propagating part of the elegant Laguerre-Gaussian laser beam in the reference plane $z = \lambda/16$. $w_0 = \lambda/2$, $n = 3$, and $\alpha = 0$. (a) $m = 0$. (b) $m = 1$. (c) $m = 2$. (d) m=3.

that of the whole laser beam. Moreover, the shape of distribution of the orbital angular momentum density of the propagating part of the elegant Laguerre-Gaussian laser beam is different from that of the whole laser beam. Therefore, the evanescent part of elegant Laguerre-Gaussian laser beam should be taken into account in the source region.

Figure 7 shows the orbital angular momentum density in the section plane $y = x$ of the propagating part (the red solid curve) and the whole laser beam (the blue solid curve) in the different observation planes. $w_0 = \lambda/2$, $n = 3$, $m = 1$, and $\alpha = 0$ in Figure 7. As $J_z(0, y, z,)$ and $J_z(x, 0, z,)$ are equal to zero, the distribution of the orbital angular momentum density in the section plane $y = x$ is examined. The observation planes are $z = \lambda/16$, $z = \lambda/2$, $z = 2\lambda$, and $z = 5\lambda$, respectively. Upon propagation, the difference between the orbital angular momentum densities of the propagating part and the whole laser beam decreases. When the ratio z/λ is large enough, the evanescent part of the orbital angular momentum density can be neglected.

4 CONCLUSIONS

Based on the method of the vectorial angular spectrum of a laser beam, an analytical expression of the electric field of the elegant Laguerre-Gaussian

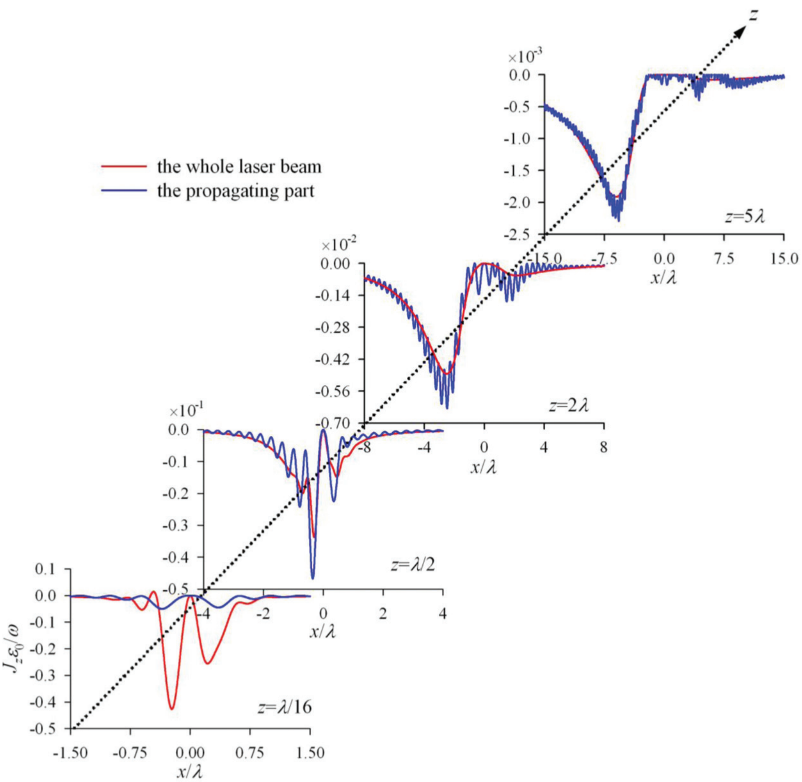

FIGURE 7
The orbital angular momentum density in the section plane $y = x$ of the propagating part (the red solid curve) and the whole laser beam (the blue solid curve) in the different observation planes. $w_0 = \lambda/2$, $n = 3$, $m = 1$, and $\alpha = 0$. (a) $z = \lambda/16$. (b) $z = \lambda/2$. (c) $z = 2\lambda$. (d) $z = 5\lambda$.

laser beam in free space is derived without any approximation. By taking the curl of the obtained electric field, the magnetic field of the elegant Laguerre–Gaussian laser beam can be obtained. By using the obtained expressions of the electromagnetic fields, the orbital angular momentum density of the elegant Laguerre-Gaussian laser beam can be accurately calculated in the source region. As the overall transverse component of the orbital angular momentum is zero, here only the longitudinal component of the orbital angular momentum density is considered. The effects of the angular mode number, the radial mode number, the linearly polarized angle as well as the beam waist width on the distribution of the orbital angular momentum density of the elegant Laguerre-Gaussian laser beam in the source region are examined. As the angular mode number increases, the magnitude of the orbital angular momentum density increases rapidly and the pattern size of the orbital angular momentum density slowly augments. With the increasing in a radial mode number, the magnitude of the orbital angular momentum density increases, but the pattern size of the orbital angular momentum density decreases. The shape of the distribution of the orbital angular momentum density is nearly insensitive to the angular and the radial mode numbers. The linearly polarized angle affects the shape, the location, and the magnitude of the distribution of the orbital angular momentum density. As the linearly polarized angle increases, the distribution of the orbital angular momentum density rotates anticlockwise and its rotation angle is the same as the linearly polarized angle. With the beam waist width increasing, the magnitude and the pattern size of the orbital angular momentum density increase, and the shape of the distribution of the orbital angular momentum density also changes.

The influence of the axial propagation distance on the distribution of the orbital angular momentum density of the elegant Laguerre-Gaussian laser beam is also investigated. Upon propagation, the profile of the distribution of orbital angular momentum density expands and the magnitude of the orbital angular momentum density decreases. Meanwhile, the shape of the distribution of the orbital angular momentum density changes obviously at first and then tends to be stable. Finally, the distribution of the orbital angular momentum density of the propagating part of the elegant Laguerre–Gaussian laser beam is compared with that of the whole laser beam. The magnitude of the orbital angular momentum density of the propagating part of the elegant Laguerre–Gaussian laser beam is far smaller than that of the whole beam. Moreover, the shape of distribution of the orbital angular momentum density of the propagating part of the elegant Laguerre–Gaussian laser beam is different from that of the whole laser beam. Upon propagation, the difference between the orbital angular momentum densities of the propagating part and the whole laser beam decreases. This research is beneficial to the optical trapping, the optical guiding, and the optical manipulation with an elegant Laguerre–Gaussian laser beam.

ACKNOWLEDGMENTS

This research was supported by the Zhejiang Provincial Natural Science Foundation of China under Grant No. LY16A040014 and the National Natural Science Foundation of China under Grant No. 11574272.

NOMENCLATURE

D_{j+1}	Parabolic cylinder function
$\mathbf{e}_x$	Unit vector in the x–direction
$\mathbf{e}_y$	Unit vector in the y–direction
$\mathbf{e}_z$	Unit vector in the z–direction

F	Faddeev function
j	Arbitrary integer
J_m	m^{th} order Bessel function of the first kind
k	Wave number (1/m)
L_n^m	Laguerre polynomial
m	Angular mode number
n	Radial mode number
w_0	Gaussian waist size (m)

Greek symbols

α	Linearly polarized angle (degree)
ε_0	Electric permittivity of vacuum (F/m)
θ	Azimuth angle (degree)
λ	Optical wavelength (m)
μ_0	Magnetic permeability of vacuum (N/A^2)
ρ	Radial coordinate (m)
ω	Angular frequency (Hz)

REFERENCES

[1] Takenaka T., Yokota M. and Fukumitsu O. Propagation of light beams beyond the paraxial approximate. *Journal of the Optical Society of America A: Optics, Image Science and Vision* **2**(6) (1985), 826–829.

[2] Bandres M.A. and Gutiérrez–Vega J.C. Higher-order complex source for elegant Laguerre–Gaussian waves. *Optics Letters* **29**(19) (2004), 2213–2215.

[3] Nasalski W. Exact elegant Laguerre–Gaussian vector wave packets. *Optics Letters* **38**(6) (2013), 809–811.

[4] Nasalski W. Vortex and anti-vortex compositions of exact elegant Laguerre-Gaussian vector beams. *Applied Physics B: Laser and Optics* **115**(2) (2014), 155–159.

[5] Borghi R. Elegant Laguerre-Gauss beams as a new tool for describing axisymmetric flattened Gaussian beams. *Journal of the Optical Society of America A: Optics, Image Science and Vision* **18**(7) (2001), 1627–1633.

[6] Porras M.A., Borghi R. and Santarsiero M. Relationship between elegant Laguerre–Gauss and Bessel-Gauss beams. *Journal of the Optical Society of America A: Optics, Image Science and Vision* **18**(1) (2001), 177–184.

[7] Zauderer E. Complex argument Hermite–Gaussian and Laguerre–Gaussian beams. *Journal of the Optical Society of America A: Optics, Image Science and Vision* **3**(4) (1986), 465–469.

[8] Saghafi S. and Sheppard C.J.R Near field and far field of elegant Hermite-Gaussian and Laguerre-Gaussian modes. *Journal of Modern Optics* 45 (10) (1998), 1999–2009.

[9] Deng D., Guo Q., Wu L. and Yang X. Propagation of radially polarized elegant light beams. *Journal of the Optical Society of America B: Optical Physics* **24**(3) (2007), 636–643.

[10] Qu J., Zhong Y., Cui Z. and Cai Y. Elegant Laguerre-Gaussian beam in a turbulent atmosphere. *Optics Communications* **283**(14) (2010), 2772–2781.

[11] Xu H., Cui Z. and Qu J. Propagation of elegant Laguerre–Gaussian beam in non–Kolmogorov turbulence. *Optics Express* **19**(22) (2011) 21163–21173.

[12] Ni Y. and Zhou G. Nonparaxial propagation of an elegant Laguerre–Gaussian beam orthogonal to the optical axis of a uniaxial crystal. *Optics Express* **20**(15) (2012), 17160–17173.

[13] Nasalski W. Elegant Hermite and Laguerre Gaussian beams at a dielectric interface. *Optica Applicata* XL(3) (2010), 615–622.

[14] Chu X. Evolution of elegant Laguerre–Gaussian beam disturbed by an opaque obstacle. *Journal of Electromagnetic Waves and Applications* **26**(13) (2012), 1749–1755.

[15] Luo S. and Lü B. Propagation of the kurtosis parameter of elegant Hermite–Gaussian and Laguerre–Gaussian beams passing through *ABCD* systems. *Optik* **113**(5) (2002), 227–231.

[16] Mei Z. The elliptical elegant Laguerre–Gaussian beam and its propagation through aligned and misaligned paraxial optical systems. *Optik* **118**(8) (2007), 361–366.

[17] Xu Y. Propagation of elegant Laguerre–Gaussian beam through a misaligned optical system. *Optics Communications* **308**(2013), 237–242.

[18] Mei Z. and Zhao D. Propagation of Laguerre–Gaussian and elegant Laguerre–Gaussian beams in apertured fractional Hankel transform systems. *Journal of the Optical Society of America A: Optics, Image Science and Vision* **21**(12) (2004), 2375–2381.

[19] Zhou G. Vectorial structure of an elegant Laguerre–Gaussian beam in the far–field regime. *Lasers in Engineering* **24**(3-4) (2012), 127–146.

[20] Gutiérrez–Vega J.C. Fractionalization of optical beams: II. Elegant Laguerre–Gaussian modes. *Optics Express* **15**(10) (2007), 6300–6313.

[21] Martinez-Castellanos I. and Gutiérrez–Vega J.C. Vortex structure of elegant Laguerre–Gaussian beams of fractional order. *Journal of the Optical Society of America A: Optics, Image Science and Vision* **30**(11) (2013), 2395–2400.

[22] April A. Nonparaxial elegant Laguerre–Gaussian beams. *Optics Letters* **33**(12) (2008), 1392–1394.

[23] Mei Z. and Gu J. Comparative studies of paraxial and nonparaxial vectorial elegant Laguerre–Gaussian beams. *Optics Express* **17**(17) (2009), 14865–14871.

[24] Wang F., Cai Y. and Korotkova O. Partially coherent standard and elegant Laguerre–Gaussian beams of all orders. *Optics Express* **17**(25) (2009), 22366–22379.

[25] Wang F., Cai Y., Eyyuboglu H.T. and Baykal Y.K. Average intensity and spreading of partially coherent standard and elegant Laguerre–Gaussian beams in turbulent atmosphere. *Progress in Electromagnetics Research* **103**(2010), 33–56.

[26] Luo H., Xu H., Cui Z. and Qu J. Beam propagation factor of partially coherent Laguerre–Gaussian beams in non–Kolmogorov turbulence. *Progress in Electromagnetics Research M* 22 (2012), 205–218.

[27] Xu H., Luo H., Cui Z. and Qu J. Polarization characteristics of partially coherent elegant Laguerre–Gaussian beams in non–Kolmogorov turbulence. *Optics and Lasers in Engineering* **50**(5) (2012), 760–766.

[28] Zhang Y., Dong Y., Wen W., Wang F. and Cai Y. Spectral shift of a partially coherent standard or elegant Laguerre–Gaussian beam in turbulent atmosphere. *Journal of Modern Optics* **60**(5) (2013), 422–430.

[29] Zhang Y., Liu L., Wang F., Cai Y., Ding C. and Pan L. Average intensity and spectral shifts of a partially coherent standard or elegant Laguerre–Gaussian beam beyond paraxial approximation. *Optical and Quantum Electronics* **46**(2) (2014), 365–379.

[30] Lopez-Mago D., Davila-Rodriguez J. and Gutiérrez–Vega J.C. Derivatives of elegant Laguerre–Gaussian beams: Vortex structure and orbital angular momentum. *Journal of Optics* **15**(12) (2013), 125709.

[31] Zhou G. and Ru G. Orbital angular momentum density of an elegant Laguerre–Gaussian beam. *Progress in Electromagnetics Research* **141**(2013), 751–768.

[32] Porras M.A. Non–paraxial vectorial moment theory of light beam propagation. *Optics Communications* **127**(1–3) (1996), 79–95.

[33] Chen C.G., Konkola P.T., Ferrera J., Heilmann R.K. and Schattenburg M.L. Analyses of vector Gaussian beam propagation and the validity of paraxial and spherical approximations. *Journal of the Optical Society of America A: Optics, Image Science and Vision* **19**(2) (2002), 404–412.

[34] Gradshteyn I.S. and Ryzhik I.M. *Table of Integrals, Series, and Products*. New York: Academic Press. 1980.

[35] Poppe G.P.M. and Wijers C.M.J. More efficient computation of the complex error function. *ACM Transactions on Mathematical Software* **16**(1) (1990), 38–46.

[36] Allen L., Beijersbergen M.W., Spreeuw R.J.C. and Woerdman J.P. Orbital angular momentum of light and the transformation of Laguerre–Gaussian laser modes. *Physical Review A (Atomic, Molecular, and Optical Physics)* **45**(11) (1992), 8185–8189.

[37] Gao C., Wei G. and Weber H. Orbital angular momentum of the laser beam and the second order intensity moments. *Science China Mathematics* **43**(12) (2000), 1306–1311.